

CASE STUDY: SEDIMENT TRANSPORT IN PROPOSED GEOMORPHIC CHANNEL FOR NAPA RIVER

By V. S. Neary,¹ Member, ASCE, S. A. Wright,² and P. Bereciartua,³ Student Members, ASCE

ABSTRACT: A model study evaluates sediment transport in a geomorphic channel proposed for restoration and flood damage reduction of an 11-km tidally influenced reach of the Napa River located in California. The model study employs the unsteady quasi-2D hydrodynamic and sediment transport model MIKE 11, the simplified marsh plain accretion model MARSH 98, and the Rouse equation to predict annual average morphological changes of the geomorphic channel. The adopted modeling approach allows for the simulation of salient sediment transport processes in a river estuary, including lateral and vertical sorting of sediments, and local flushing of fine cohesive and noncohesive sediments during flooding. Accretion rates, particularly within the marsh plain terrace of the multistage channel, are found to be within acceptable limits for project maintenance and ecosystem restoration purposes. This enhanced 1D modeling approach may offer a viable and cost-effective alternative compared to fully 2D and 3D models, with relatively less model set-up and run-time requirements.

INTRODUCTION

A model study evaluates sediment transport in a geomorphic channel proposed for restoration and flood damage reduction of an 11-km tidally influenced reach of the Napa River located in California. The project reach (Fig. 1) lies within the northern limit of the historic brackish tidal marshlands of the Napa River estuary, where alluvial floodplain transitions to estuarine tidal marsh. The Napa River drains a 1,103 km² area within the California Coast Ranges, discharging to the San Pablo Bay. The lower 28 km of the river's 80.5-km length is subject to tidal influence, which extends to Trancas Road. Within this portion of the river, flood levees and navigational dredging have led to an artificially deepened channel that prevents episodic flooding of historic floodplain and tidal marsh. These impacts have also prevented daily tidal flooding, which once supplied brackish water and nutrients to support these rich ecosystems. Filling and general encroachment within the floodplain has further confined the flood flows causing channel degradation. At the oxbow meander, the raising of the floodplain with artificial fill has prevented historic overflows at the neck of the oxbow meander.

Flooding has been a chronic problem along the Napa River, causing the loss of at least three lives and more than \$540 million in property damage since 1960. Three times in the last 22 years the county voted down proposals by the U.S. Army Corps of Engineers to construct traditional flood control works, including a cutoff channel, levees, and flood walls. In 1995 a group of community-based organizations, with the support of the Napa County Flood Control District and the Corps, came together to develop an alternative plan. This community-based coalition, supported by technical consultants and local and state resource agencies, proposed an approach, called "The Living River Strategy" (Community 1996), which provided for flood protection and river restoration. In March 1998, Napa residents voted for a half-percent increase in the

local sales tax, which was required to construct the estimated \$220 million project. The project has been described as a "radical" and "unique" approach (Doyle 2000; Ellison 2000) and has received considerable media attention, including coverage by ABC News and *The New York Times* (Egan 1998). It restores >650 acres of highly valued wetlands and protects 2,700 homes, 350 businesses, and >50 public properties from flood damages with an estimated annual cost of \$26 million [Federal Emergency Management Agency (FEMA) 2000].

The Living River Strategy was the basis for the design of a geomorphic channel that balanced flood-damage-reduction needs for the city of Napa, continued navigational use, and restoration of historic tidal marsh and floodplains. Refer to Neary et al. (1996) for details. The term "geomorphic" was coined to describe the channel because the main channel design features were developed using principles of tidal and fluvial geomorphology, with the underlying assumption that restoring physical geomorphic features of the channel would provide the foundation for ecological restoration.

The two key features of the geomorphic channel design, illustrated in Fig. 2, include a raised-bed cutoff channel at the neck of the oxbow meander referred to locally as the "dry bypass," and a widened terraced channel in the lower reach, which is relatively less encroached upon. The dry bypass profile restores the historic overflows at the neck of the oxbow meander. Also, unlike conventional flood control cutoff channels, it maintains the existing conditions' energy slope for more frequent flood events with discharges at or less than the dominant discharge, thereby maintaining longitudinal sediment equilibrium and preserving the present oxbow meander channel. The dominant discharge that was used to set the bank-full flow elevations is the effective sediment-transporting discharge, which was calculated using the magnitude-frequency analysis introduced by Wolman and Miller (1960). The terraced channel was designed with the following features: (1) low-flow channel maintained by tidal scour and navigation dredging; (2) widened bank-full flow channel maintained by dominant discharge; (3) marshplain terrace that restores main-channel-tidal-marsh processes; and (4) floodplain terrace lowered to the dominant discharge water level so that it restores main-channel-alluvial-floodplain interaction.

The main objective of the modeling study was to calculate sediment erosion, transport, and deposition locally at three separate areas within the geomorphic channel cross section (the main channel, marshplain terrace, and floodplain terrace) from River Station 55.7–60.2 km (Fig. 2). Evaluation of deposition in the marshplain terrace was of particular concern. The setting of the marshplain terrace at the mean tide level

¹Asst. Prof., Dept. of Civ. and Envir. Engrg., Tennessee Technol. Univ., Cookeville, TN 38505-0001. E-mail: vneary@tntech.edu

²Grad. Res. Asst., St. Anthony Fall Lab., Univ. of Minnesota, Minneapolis, MN 55455.

³Grad. Res. Asst., Dept. of Civ. and Envir. Engrg., Univ. of California at Berkeley, CA 94720.

Note. Discussion open until April 1, 2002. To extend the closing date one month, a written request must be filed with the ASCE Manager of Journals. The manuscript for this paper was submitted for review and possible publication on April 24, 2000; revised August 6, 2001. This paper is part of the *Journal of Hydraulic Engineering*, Vol. 127, No. 11, November, 2001. ©ASCE, ISSN 0733-9429/01/0011-0901-0910/\$8.00 + \$.50 per page. Paper No. 22306.

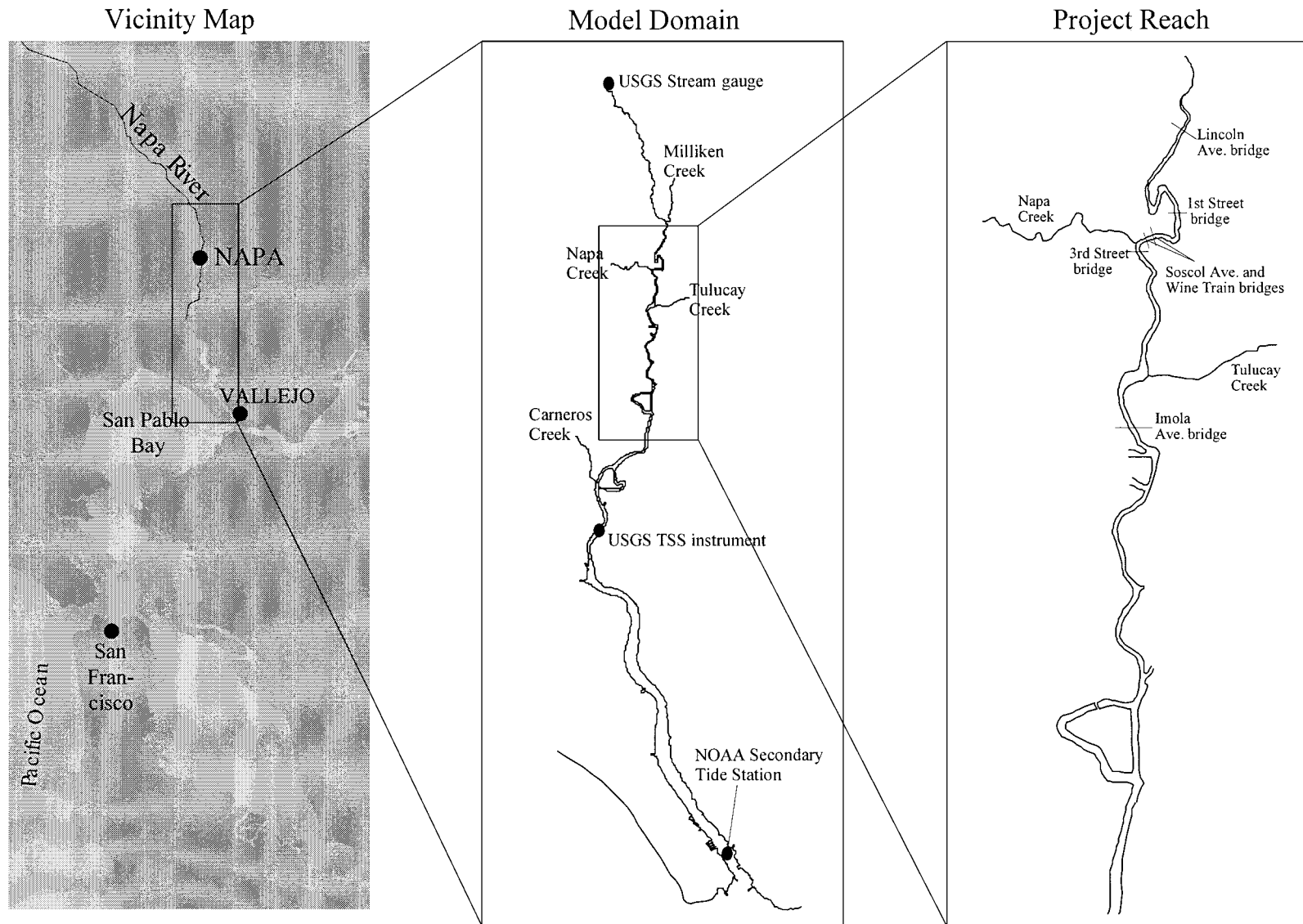


FIG. 1. Napa River Vicinity Map, Model Domain, and Project Reach

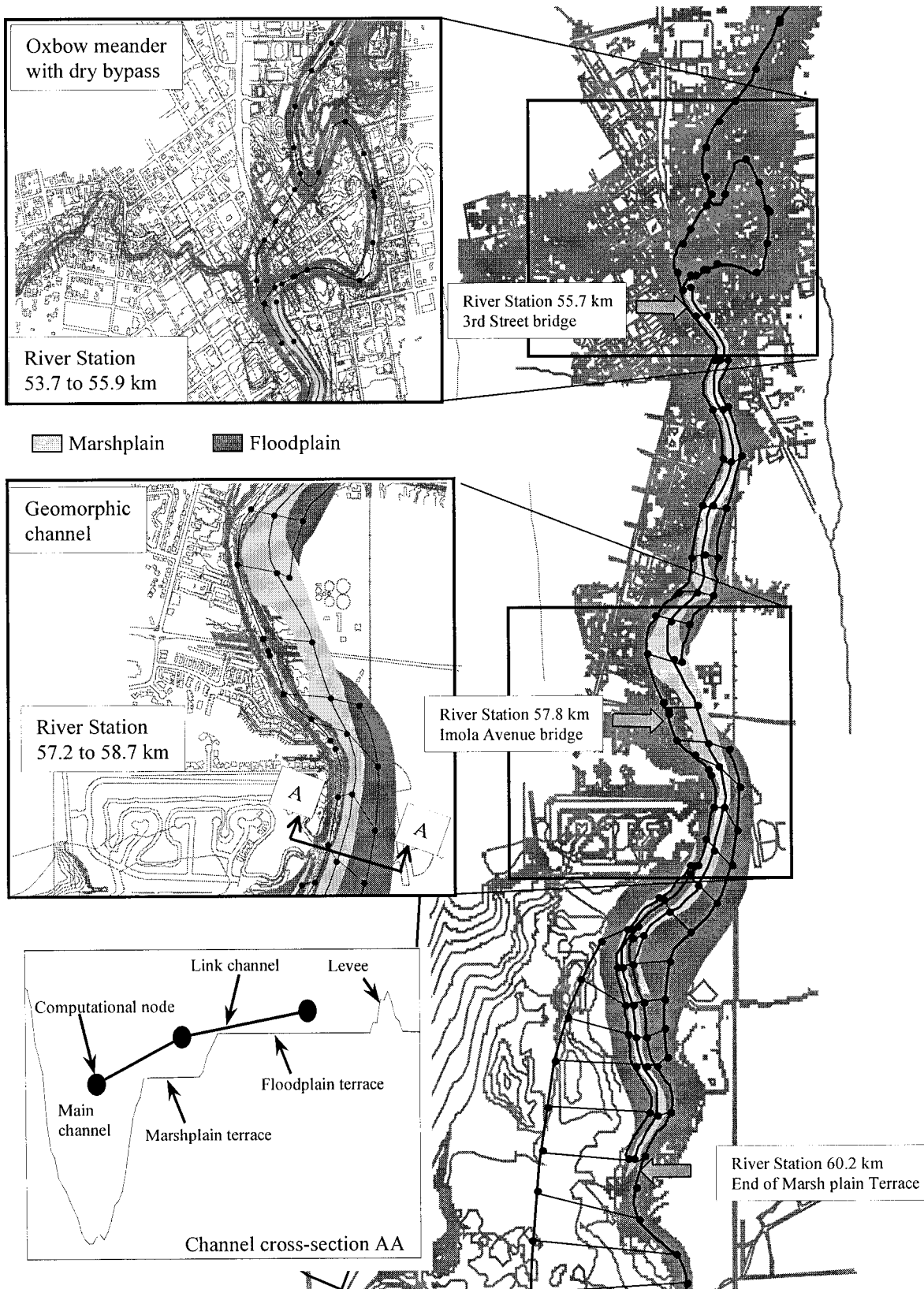


FIG. 2. Geomorphic Channel and Computational Grid

was a departure from the geomorphic design principles (Neary et al. 1996) because this terrace is at equilibrium at mean high water. Consequently, fine cohesive and noncohesive sediment deposition in this area is expected. High deposition rates of 60 mm/year or more would quickly reduce the flood convey-

ance performance of the channel, requiring maintenance approximately every 5–10 years and severely affecting restored intertidal habitat. Other important objectives related to the geomorphic stability of the channel included an assessment of the impact of the dry bypass channel on longitudinal channel

stability, assessment of potential upstream and downstream impacts, and identification of problem areas of excessive erosion or deposition.

HYDRODYNAMIC AND SEDIMENT TRANSPORT MODELS

The sediment transport regime of a river estuary, where both fluvial and tidal sedimentation occurs, is complex and presented several challenges that factored in model selection and the modeling approach adopted in this study. Sediment core samples from previous sediment studies [Water Engineering & Technology, Inc. (WET) 1990; Applied Water Engineers, Inc. (AWE) 1996] indicated that sediment was laterally and vertically heterogeneous. Bank material throughout the project reach consisted of cohesive alluvial fan sediments and tidally transported cohesive bay muds. In contrast, bed material consisted of noncohesive coarse to fine sands, with localized gravel deposits in the upper portion of the project reach.

The presence of fine cohesive sediments on the banks was expected because of the combined effect of relatively lower bottom shear stresses in these areas compared to the channel bed and the lower suspended sediment concentrations of coarser materials transported higher in the water column. It was therefore necessary that the model study account for cohesive sediment transport, which was expected to dominate in the terraced areas of the proposed channel, as well as noncohesive sediment transport dominating in the deeper main channel. Also, it was important that the study account for the lateral variation in bottom shear stress that is partly responsible for the observed sediment sorting across the existing channel. This analysis was particularly important for evaluating a multistage channel that included marshplain and floodplain terraces set at higher elevations.

The MIKE 11 Model (*MIKE 11* 1995), an unsteady quasi-2D hydrodynamic model with noncohesive sediment transport (NST) and cohesive sediment transport (CST) submodels, was the main model selected to address the study objectives. The NST model was employed to simulate transport of coarse sediments, with grain sizes greater than or equal to 0.062 mm in diameter, as bed and suspended load. The CST model was employed to simulate fine grain transport with diameters <0.062 mm. One-dimensional models, such as HEC-6, cannot explicitly resolve lateral variations in bottom shear stress, vertical variations in suspended sediment load, and the resultant variation of sediment properties and transport processes in the channel cross section. As explained below, lateral and vertical heterogeneities were resolved in this study by constructing a quasi-2D grid and employing the Rouse equation with the log-law velocity distribution assumption. Multiple-dimensional models were considered to be too computationally intensive in terms of model set-up and run-time requirements. Furthermore, vertical and transverse mixing due to density- and wind-driven currents and tidal trapping was considered to be relatively minor compared to shear-driven longitudinal mixing, particularly within the project reach. The channel is narrow and curved, resulting in minimal fetch. Gravitational circulation, due to density stratification, has been observed at the location of the USGS total suspended solids (TSS) instrument for freshwater pulses in the range from approximately 5 to 15 m³/s (Warner et al. 1999), but these flows are well below the range of the dominant discharge of approximately 360 m³/s. A quasi-2D model was judged to be appropriate for resolving the salient sediment transport processes required to address the study objectives, as well as a convenient and relatively simple model with which to work.

The MIKE 11 hydrodynamic model solves the Saint-Venant equations by employing a six-point implicit staggered-grid finite-difference scheme developed by Abbott and Ionescu

(1967). The numerical scheme is adapted for application to looped networks and quasi-2D flow simulations on floodplains. The NST model solves the sediment continuity equation

$$(1 - \epsilon) \frac{\partial(Wz_b)}{\partial t} + \frac{\partial Q_s}{\partial x} = 0 \quad (1)$$

where z_b = bed level; Q_s = sediment discharge; ϵ = sediment porosity; and W = width of cross section at water surface. The model was run in a morphological mode, meaning that the bed level is updated at every time step while running the hydrodynamic and NST models in tandem. The van Rijn model, based on model validation results, was determined to be the most accurate model for calculating bed and suspended load transport. Model validation also indicated that the use of the D_{50} particle size of the bed material as the single representative grain size was sufficient (Neary et al. 1997). Therefore, the option to model different grain size fractions was not adopted.

The CST model solves the advection-dispersion equation

$$\frac{\partial AC}{\partial t} + \frac{\partial QC}{\partial x} - \frac{\partial}{\partial x} \left(AK \frac{\partial C}{\partial x} \right) = S_e - S_d \quad (2)$$

where Q = water discharge; A = cross-sectional flow area; C = cross-sectional average sediment concentration; K = dispersion coefficient; S_e = erosion (resuspension) flux; and S_d = deposition flux. The CST model predicts the variation of sediment concentration in space and time, as well as accumulated sediment deposits over the simulation time. At the time of this study, the CST model was not coupled with the NST model, so the CST and NST model simulations were done separately.

Erosion flux is expressed by the equation

$$S_e = \frac{M^*}{D} \left[1 - \left(\frac{U}{U_{ce}} \right)^2 \right], \quad U \geq U_{ce} \quad (3)$$

where M^* = bed erodibility; D = flow depth; U = cross-sectional average flow velocity; and U_{ce} = critical erosion velocity. Deposition flux is expressed by the equation

$$S_d = \frac{wC}{D^*} \left[1 - \left(\frac{U}{U_{cd}} \right)^2 \right], \quad U \leq U_{cd} \quad (4)$$

where w = mean settling velocity of suspended particles; D^* = average depth through which particles settle; and U_{cd} = critical deposition velocity.

Lateral and vertical heterogeneities were resolved in this study by constructing a quasi-2D computational grid and employing the Rouse equation with the log-law velocity distribution assumption. The computational grid consisted of separate flow paths (branches) representing the main channel, marshplain terrace, floodplain terrace, and dry bypass, as shown in Fig. 2. Link channels were used to connect these different branches, forming a quasi-2D grid that accounts for the variation of hydrodynamic parameters (i.e., velocity, depth, and bottom shear stress) and, hence, lateral variations in erosion, deposition, and sediment transport across the channel cross section. Their use for simulating flow and sediment exchange between the main channel, marshplain, and floodplain can be problematic, as pointed out by Cunge et al. (1980). This is especially the case for minor flood events, such as the 2-year flood, where the channel flow is only slightly higher than bank full and the floodplain is only partially inundated. It is also more difficult to use link channels when there are no clearly defined locations for overflow, as was the case for the terraced channel in the lower project reach.

The application of link channels adopted herein followed the recommendations by Cunge et al. (1980). Link channels were spaced close enough together so that the drop in the water level between them is small. The flow through the link

channels was regulated by a single rectangular weir whose crest elevation is the same as the average bank elevation along the channel length between two longitudinal computational points. Sediment from the main branch to the parallel branches representing the marshplain and floodplain terraces was distributed according to coefficients in the MIKE 11 model. These coefficients were determined external to the MIKE 11 model by numerical integration, where the ratio of sediment discharge above the terrace elevation q_{st} relative to the total q_s above the reference level a is given by

$$\frac{q_{st}}{q_s} = \frac{\int_a^d cu \, dz}{\int_a^d cu \, dz} \quad (5)$$

The local sediment concentration was calculated by the Rouse formula (ASCE 1975). The log-law was assumed for the vertical velocity distribution.

The model domain encompassed the lower 35 km of the Napa River estuary, which extended beyond the 11-km study reach in the upstream and downstream directions. The upstream boundary corresponded with the location of a USGS gauge station at Oak Knoll (river chainage 45.33 km), where water stage was recorded continuously every 15 min and where a stage-discharge and sediment-discharge rating were established by previous studies (AWE 1996). The downstream boundary corresponded with the location of a secondary tidal station at Mare Island Strait (river chainage 80.53 km), established by the National Oceanic and Atmospheric Administration (NOAA) for the prediction of tidal stages recorded continuously every 15 min based on measured tidal stage at the primary tidal station located in the San Pablo Bay. Within the model domain at Brazos Bridge (river chainage 67.64 km), TSS concentration was measured 61 cm above the channel bed by the USGS every 10 min over a 3-month period in 1997 (Warner et al. 1999).

The existing and proposed channel bathymetries were based on 82 channel cross sections. The Napa County Resource Conservation District measured 24 cross sections within the upper 6 km of the model domain in 1995. The U.S. Army Corps of Engineers surveyed 42 cross sections within the 11-km project reach in 1989. Sixteen cross sections in the lower 18 km of the model domain were derived from soundings (Neary et al. 1996). The computational grid for existing channel condition consisted of 91 h -nodes and 90 Q -nodes. For the project conditions, it included seven branches representing the main channel, marshplains, and floodplains, with a combined total of 137 h -nodes and 127 Q -nodes. For both conditions, the h -grid nodes generally correspond with the location of the surveyed channel cross sections spaced approximately every 200 m in the project reach. However, in the lower 18-km reach, where fewer cross sections were available, h -nodes were located a maximum of 1,000 m apart.

A simplified marshplain accretion model, MARSH 98 (DeTemple 1998), based on the model originally developed by Krone (1987), was employed to predict the long-term evolution of marshplain terrace elevations due to tidal action and a 2-mm/year sea level rise. This estimate of sea level rise is based on observed trends for San Francisco over the twentieth century [Intergovernmental Panel on Climate Change (IPPC) 1995]. MARSH 98 is a vertical 1D model that solves the conservation of mass of suspended sediment over a unit area of marsh expressed

$$(\eta - z) \frac{dC}{dt} = -wC - (C_* - C) \frac{d\eta}{dt} \quad (6)$$

where $C_* = C_0$ on the flood tide, $d\eta/dt > 0$, and $C_* = C$ on the ebb tide, $d\eta/dt \leq 0$; η = tide elevation; z = marshplain elevation; w = median settling velocity of suspended particles; and C_0 = concentration of suspended sediment in flooding waters. The median settling velocity by weight was expressed by Krone (1962) as $w = \beta C^{4/3}$, where $\beta = 110$ for w in centimeters per second and C in grams per cubic centimeters. The deposition during inundation can be approximated by

$$\Delta z = \frac{\int_t wC}{C_d} dt \quad (7)$$

where C_d = dry density of inorganic component of the marsh substrate. A typical value of C_d is 0.56 g/cm³ for salt marsh with a dry density of composite substrate 0.67 g/cm³ and an organic content of 16.4%.

MODEL CALIBRATION

The hydrodynamic and sediment transport models were calibrated by comparing model simulation results for the existing channel conditions with available measured data and adjusting model parameters, within reasonable ranges, to give best agreement. The HD model was calibrated to predict observed high water marks taken for a 1995 flood event within the 11-km project reach. The main parameter adjusted for model calibration was Manning's n . Local energy loss coefficients, for flow through bridge sections, were also adjusted. The calibration resulted in physically acceptable Manning's n values varying approximately linearly from $n = 0.037$ at Oak Knoll to $n = 0.031$ at Mare Island Strait. The decrease in Manning's n reflects the fact that the lower reach is relatively straight and prismatic compared to the upper reach. The calibrated model was then validated with observed high water marks recorded for a 1997 flood event. For both simulations, discharge Q time series collected at the USGS gauge station at Oak Knoll were used as the upstream boundary condition. Tidal stage h time series collected at the NOAA secondary tidal station at Mare Island Strait served as the downstream boundary condition. Tributary inflow time series for both simulation periods were derived by drainage area proration (Neary et al. 1996).

The results of the HD model calibration and validation are shown in Fig. 3. Comparison between computed and observed high water marks for both the 1995 and the 1997 flood events indicate good agreement. High water marks at Lincoln Avenue Bridge and First Street are most likely greater than computed as a result of the problem of deriving loss coefficients at bridges to reflect all possible conditions. These coefficients can vary substantially from one flood event to another.

The NST model was validated with observed changes in laterally averaged bed level at six cross sections within the project reach over 8 years between 1989 and 1997. At these cross-sections, soundings had recently been recorded in 1997. The representative grain size was adjusted longitudinally according to bed samples taken in 1989 (WET 1990), from $D_{50} = 6$ mm at Oak Knoll to approximately $D_{50} = 1$ mm through the project reach and approximately $D_{50} = 0.2$ mm at the downstream portion of the model domain. The NST model was run with the HD model in morphological mode so that the bed level was updated with velocity and depth at every time step. Hydrodynamic boundary conditions were imposed as described previously with the addition of a sediment inflow boundary condition, derived by employing the sediment rating curve established at Oak Knoll, for Napa River and tributaries entering the model domain. Fig. 4 compares NST model predictions of bed level changes from 1989 to 1997 with observed changes. The comparison, albeit at only six monitoring stations, shows reasonably good agreement considering the in-

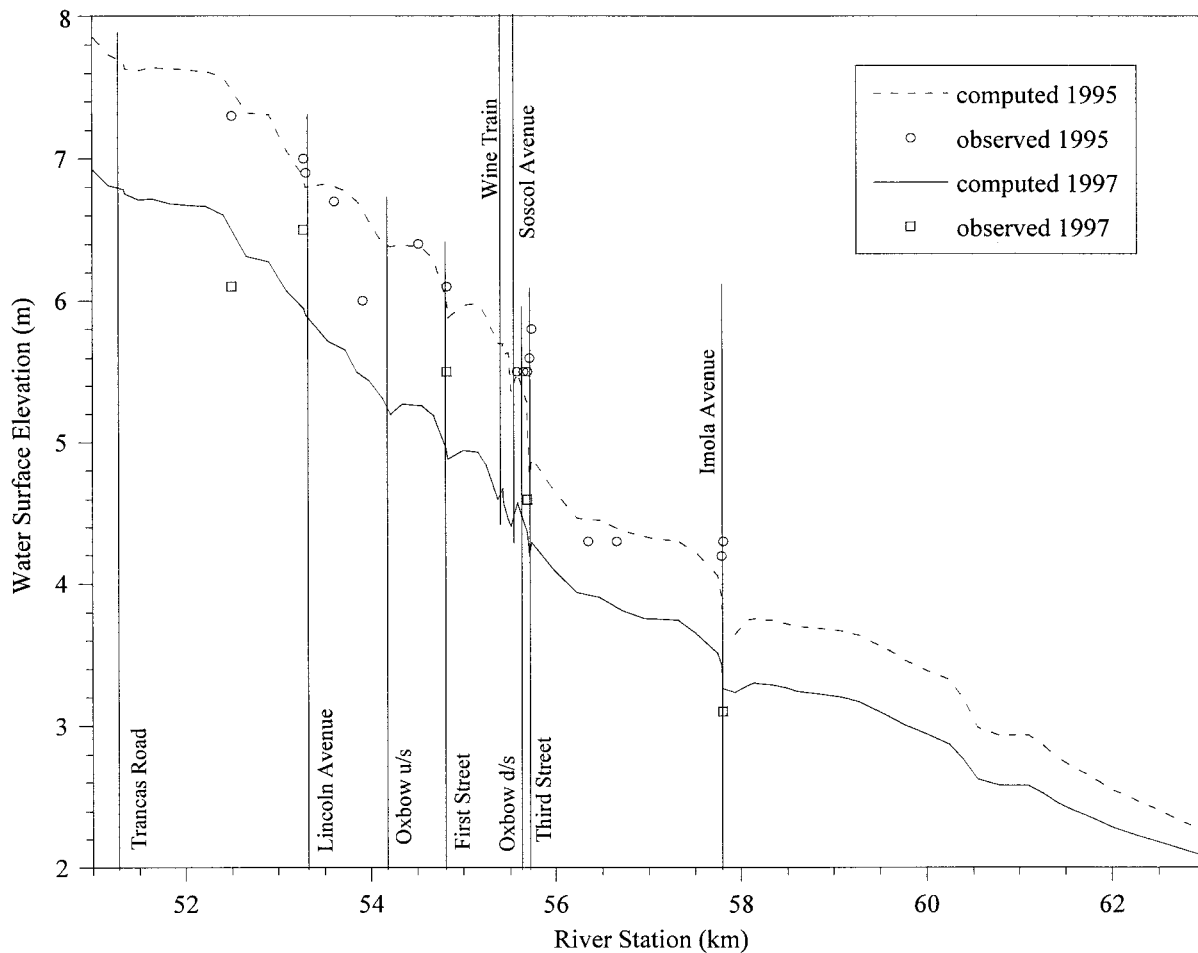


FIG. 3. Calibration and Validation of Hydrodynamic Model for 1995 and 1997 Events

herent challenges of predicting channel morphology over this long a period. The model predicts approximately 0.4 m more degradation than observed at River Stations 58.6 and 59.6 km, but it was decided that this did not warrant adjustment of the local D_{50} value obtained from field measurements.

The CST model was calibrated over a 60-day period that included several flood events in January 1997. The number of variables in the CST model and scarcity of field measurements of these variables typically makes calibration a difficult exercise. Model variables included the longitudinal dispersion coefficient K , cohesive sediment floc size FS , threshold velocities for deposition U_{cd} and erosion U_{ce} , and bed erodibility coefficient M^* . The variables FS , U_{cd} , U_{ce} , and M^* were adjusted, but within the ranges previously determined by field and experimental investigations. These ranges and the adopted values are summarized in Table 1. Values for the dispersion coefficient were calculated based on the expression

$$K = 0.011U^2W^2/DU^* \quad (8)$$

where U = cross-sectional average velocity; W = channel width; D = flow depth; and U^* = shear velocity (Fisher et al. 1979). Flow parameters for calculating the dispersion coefficient were based on the effective sediment-transporting discharge (Neary et al. 1997). Dispersion coefficients varied from $K = 200 \text{ m}^2/\text{s}$ within the upstream reach to $K = 100 \text{ m}^2/\text{s}$ in the project reach and $K = 25 \text{ m}^2/\text{s}$ in the lower reach. Model boundary conditions included sediment inflow at Oak Knoll, based on a wash load rating curve previously formulated (AWE 1996), and an open boundary condition downstream at Brazos Bridge, based on the measured TSS time series (Warner et al. 1999). As an open boundary condition, the model imposes measured TSS concentration data during periods of

inflow (flood tide) and calculates TSS concentration during periods of outflow (ebb tide). Therefore the model is calibrated during periods of outflow only.

Fig. 5 compares time series of predicted and measured suspended sediment concentration through a period of severe flooding in 1997. Comparison indicates reasonable agreement and demonstrates the model's ability to simulate resuspension for high river flows and relatively lower tidal flows for the adopted parameter settings. The model does exhibit a tendency to lag high concentrations following floods. However, attempts to calibrate model parameters within their designated ranges to mitigate this effect were unsuccessful. Despite this problem, the model performance was considered adequate for the purpose of evaluating project conditions.

MODEL SIMULATIONS OF PROJECT CONDITIONS

The adopted quasi-2D grid configuration accounted for the lateral heterogeneities in flow properties as expected. For the 100-year flood, velocities within the main channel, marshplain, and floodplain of a representative cross section were $U = 1.91$, 1.34 , and 0.15 m/s , respectively, compared to an average velocity of 1.42 m/s if the cross section were treated as a single compound channel (Fig. 2). The Rouse equation indicated a nearly uniform vertical distribution of fine sediments in the silt/clay size range ($D_{50} < 0.062 \text{ mm}$). However, nonuniform distributions were observed for sediments in the coarse to fine sand range ($D_{50} \geq 0.062 \text{ mm}$). The degree of nonuniformity resulting from respective 100-year and 2-year floods, given the D_{50} of the bed material, is shown in Fig. 6. As expected, the analysis indicates that the coarser bed material is only suspended into the flow regions at the marsh- and floodplain lev-

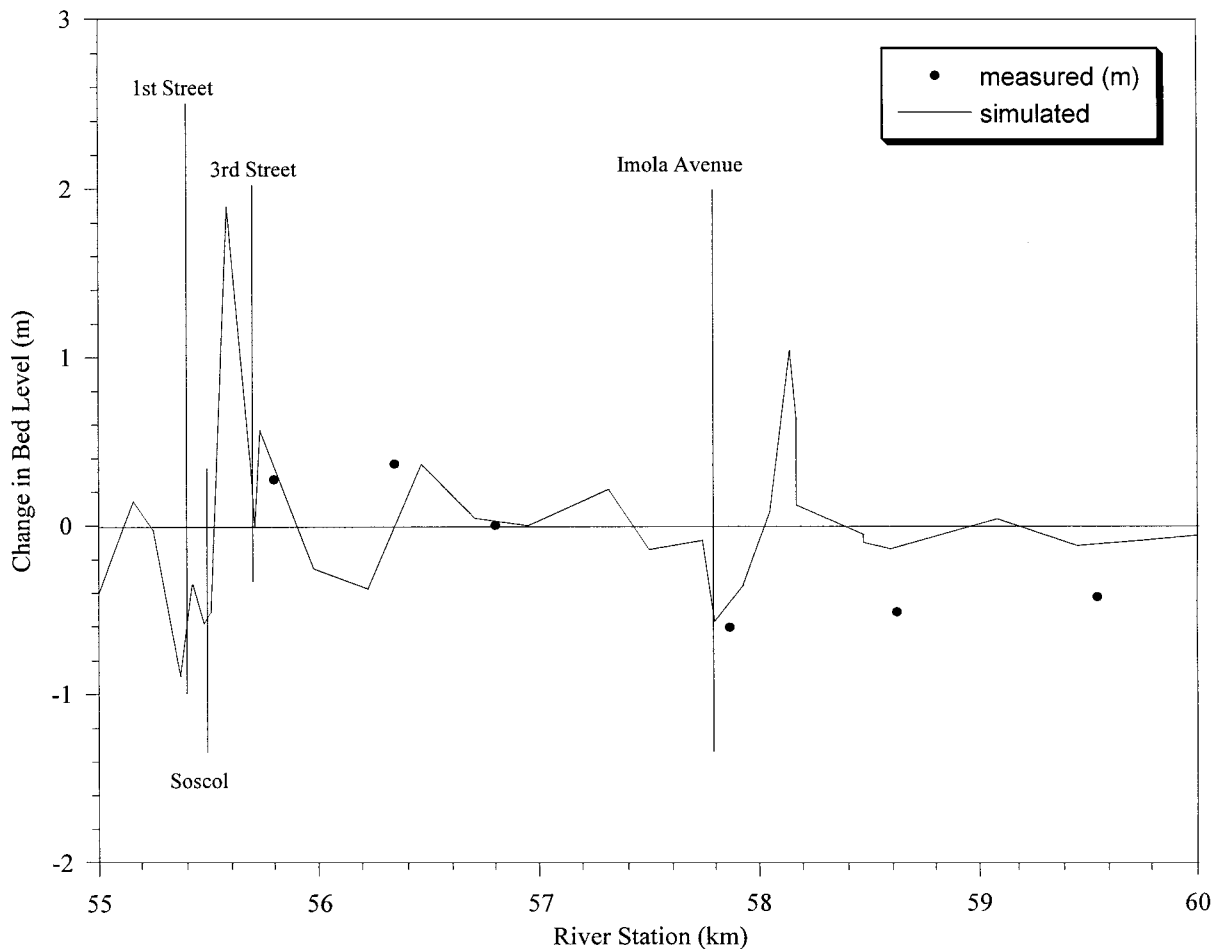


FIG. 4. Comparison of Measured and Simulated Bed Level Changes between 1989 and 1997

els for significant flood events. The percentage of noncohesive coarse to fine sand sediment transport at the marshplain terrace elevation ranged from 1% for the 2-year flood to 12% for the 100-year flood. At the floodplain terrace elevation, the percentage ranged from 0% for the 2-year flood to 4% for the 100-year flood.

Average annual changes in the geomorphic channel morphology due to fluvial sedimentation processes were calculated by statistically weighting bed level changes predicted by the MIKE 11 NST and CST submodels based on recurrence frequencies of the 100-, 55-, 10-, 5-, and 2-year flood events. Peak discharges corresponding to these return periods, and for the 1995 and 1997 floods, are provided in Table 2. Average annual changes due to fluvial sedimentation were added to the predicted annual accretion rates caused by tidal sedimentation, calculated using the simplified marsh accretion model, to determine a total average annual change. Annual morphological changes resulting from fluvial sedimentation are shown in Fig. 7. Sediment accretion within the marshplain and floodplain terraces due to fluvial sedimentation is fairly variable, ranging from 5 to 50 mm/year along the marshplain terrace and from zero to 39 mm/year along the floodplain terrace. Significant rates of accretion, >30 mm/year, are very localized. Results from the simplified marsh accretion model indicate that tidal sedimentation will cause an additional increase in elevation of 5 mm/year within the marshplain terrace. Accretion rates of 60 mm/year or more, which would require excessive maintenance, were not predicted at any location. The marsh accretion simulation assumes an average sediment concentration of 50 mg/L due to tidal action. This is a conservative estimate based on the TSS measurements in the lower portion of the project reach (Warner et al. 1999) and assuming a 2 mm/year sea level

rise over the next century (IPPC 1995). The NST model predicted little deposition on the marsh- and floodplains as expected from the Rouse analysis. It reproduced expected trends in the main channel morphology, such as erosion at channel constrictions (e.g., bridges) followed by deposition just downstream. For the 100-year flood, erosion increases for project conditions both upstream and downstream of the bypass. However, deposition in the oxbow meander occurs. The bypass remains dry for floods with return periods of approximately 2 years (the dominant discharge) or less, maintaining the longitudinal stability of the channel.

CONCLUSIONS

The adopted modeling approach is found to be well suited for dealing with the complexity of the sedimentation processes occurring within the project reach as well as the complexities of a multistage channel design. It allows for the simulation of salient sediment transport processes in a river estuary that cause lateral and vertical, as well as longitudinal, sorting of sediments. This enhanced 1D modeling approach may offer a viable and cost-effective alternative compared to fully 2D and 3D models, with relatively less model set-up and run-time requirements.

Model results indicate that overall the project channel will not require excessive maintenance. Accretion rates of 60 mm/year or more, which could compromise restoration objectives, were not predicted. However, significant rates of accretion, >30 mm/year, were found within the marsh- and floodplains but were very localized. Also, several areas in the main channel were found to have significant erosion or deposition, >1 m for a 100-year event. Monitoring in these areas, as well as

TABLE 1. CST Model Parameters

Property	Minimum value	Maximum value	Adopted value	Reference
Flock size FS (m)	0.04	0.180	0.08	Krone (1962), Gibbs (1987)
Critical velocity of deposition U_{cd} (m/s)	0.03	0.1	0.1	Krone (1962), McDonnald and Cheng (1997)
Critical velocity of erosion U_{ce} (m/s)	0.3	1	0.8	McDonnald and Cheng (1997), van Rijn (1989)
Erodibility coefficient M^* (g/m^2s)	0.001	0.4	0.01	McDonnald and Cheng (1997), van Rijn (1989)

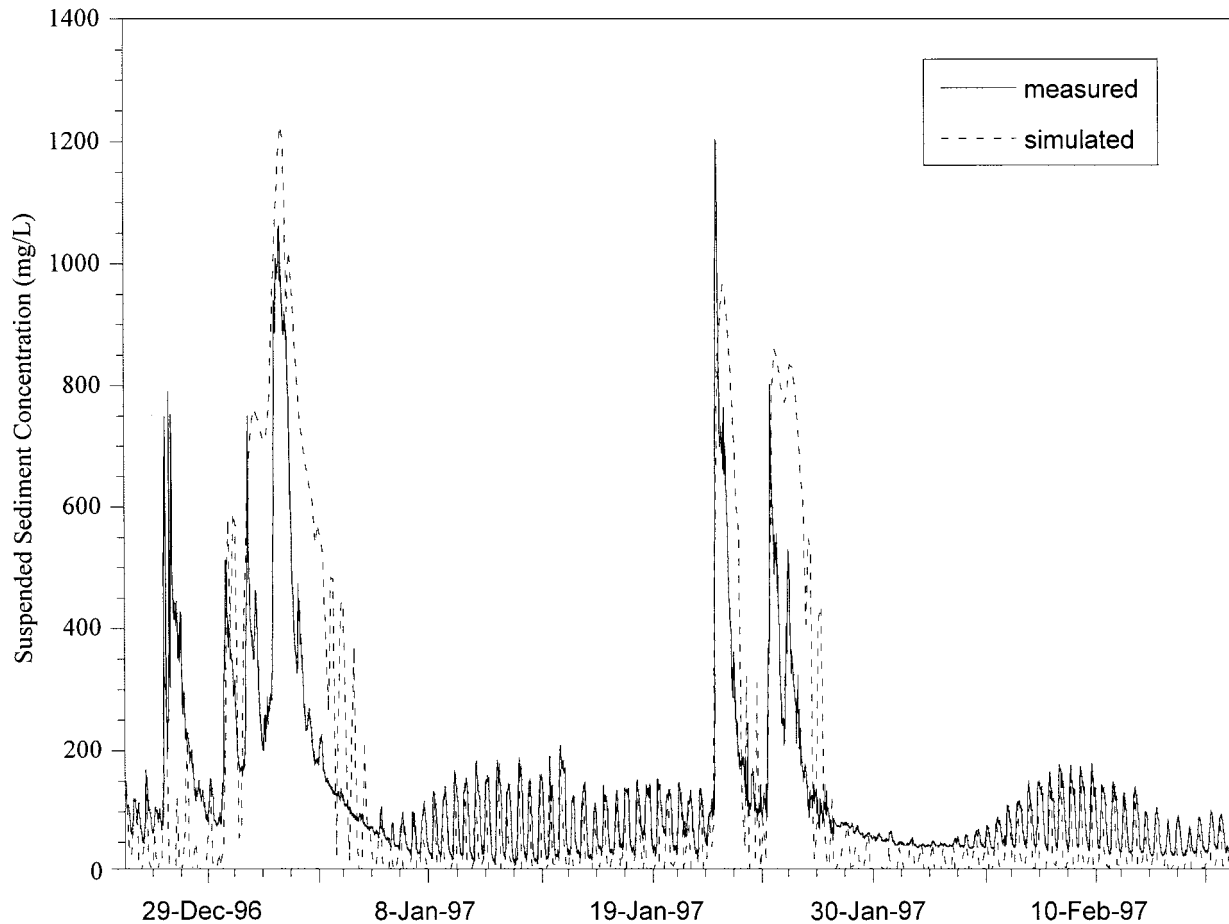


FIG. 5. Comparison between Measured and Simulated Suspended Sediment Concentration for 1997 Flood Event

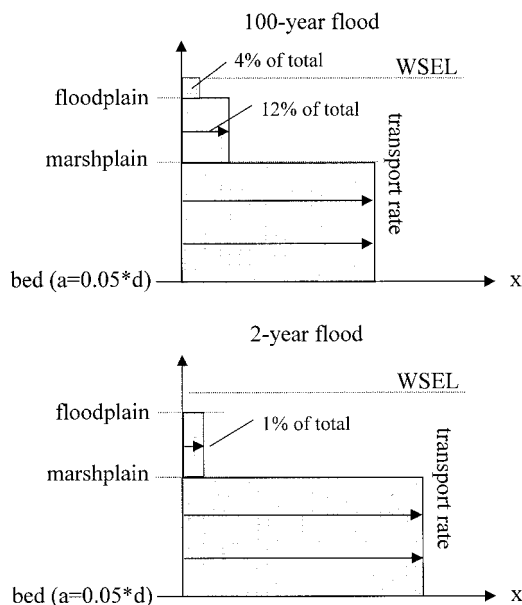


FIG. 6. Typical Noncohesive Suspended Sediment Profiles

consideration for additional bank protection in erosion-prone areas, is recommended as part of a comprehensive performance maintenance program. Continued collection of hydrodynamic, sediment transport, and morphological data after the project is constructed is recommended for improving the predictive capabilities of the model for project conditions.

Proper interpretation of the modeling results needs to consider some of the key assumptions inherent in the modeling approach adopted. Averaging flow and sediment properties within the main channel, marshplain, and floodplain means that lateral variations in sedimentation rates within each of these areas are not resolved. This limitation should not greatly

TABLE 2. Napa River Flood Magnitudes

Return period/event	Peak discharge (m^3/s)
2 year	360
5 year	490
10 year	600
55 year	830
100 year	930
1995	920
1997	660

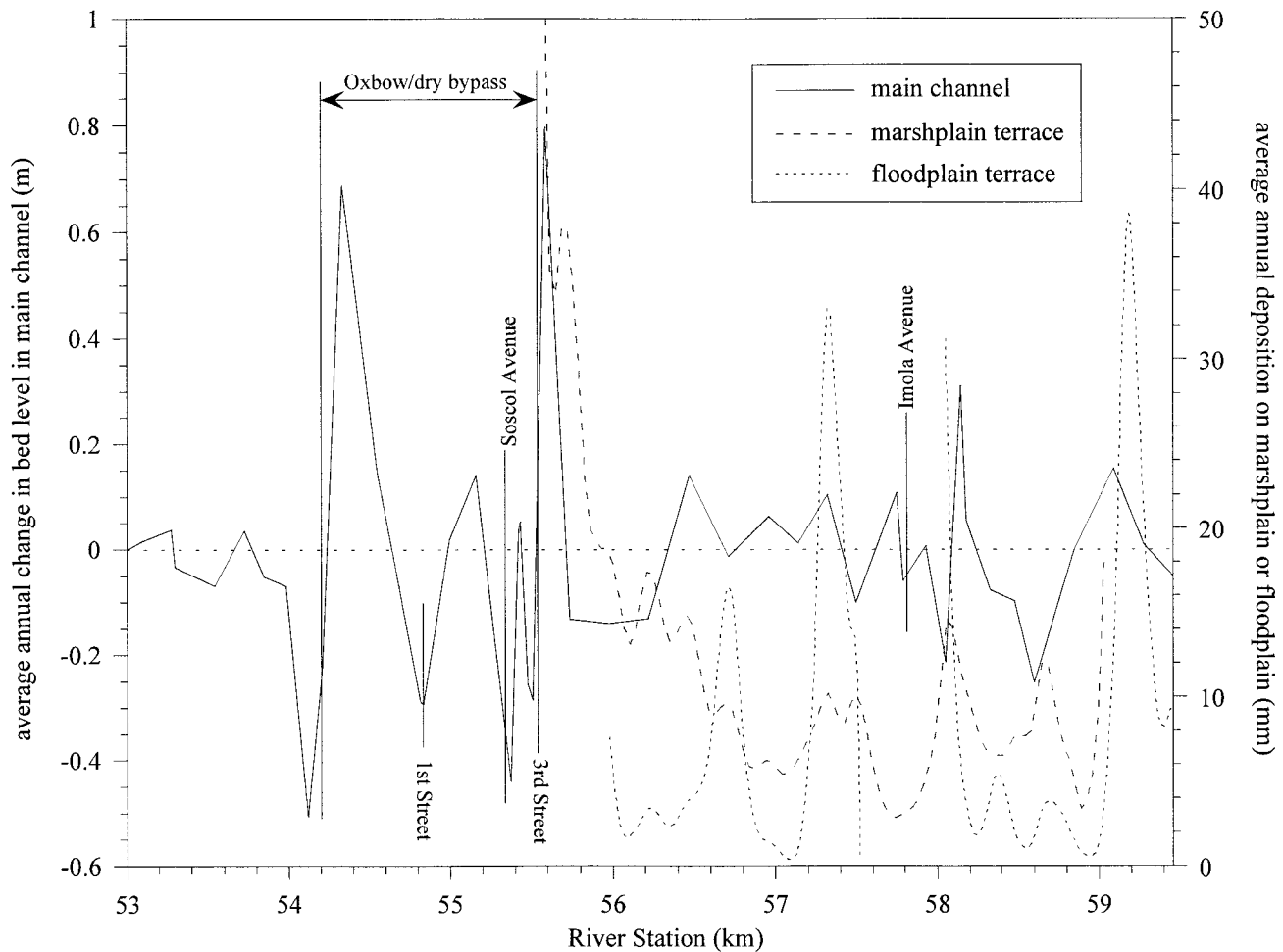


FIG. 7. Predicted Average Annual Bed Level Changes in Main Channel and Deposition Levels on Marshplain and Floodplain Terraces

impair the assessment of sedimentation effects on flood conveyance performance. However, it may not provide the degree of resolution ultimately desired by ecologists to assess impacts on intertidal habitat. This is particularly the case for assessing sedimentation rates on sloped areas where there is a significant gradient of plant zonation patterns.

The modeling approach also assumes that both fluvial and tidal sedimentation processes are important in the project reach and that they act independently of one another. Fluvial sedimentation is caused by the cumulative effect of random episodic floods and can result in significant morphological changes over a short time period; whereas, tidal sedimentation is caused by predictable periodic flows and can result in small morphological changes but occurs continuously, which can add up to significant changes in the long term. The approach adopted in this study, evaluating these processes separately and then summing sedimentation rates, should give conservative estimates. Ascertaining the relative contribution of fluvial and tidal sedimentation processes in a river estuary, and how these processes interact, is a topic for further research.

ACKNOWLEDGMENTS

This study was completed in 1997 while the writers were employed at Philip Williams & Associates, Ltd. The writers thank the following for their valuable contributions: Philip Williams of Philip Williams & Associates, Ltd.; Peter Goodwin of the University of Idaho, Moscow, Idaho; Larry Dacus and Greg Kukas of the U.S. Army Corps of Engineers, Sacramento District; John Warner and Geoff Schladow of the University of California at Davis; David Schoellhamer, USGS; and Morten Rungo and Hans Engrob of DHI Water and Environment.

REFERENCES

- Applied Water Engineers, Inc. (AWE). (1996). "Napa River sediment engineering and channel stability analysis project condition." *Final Rep. Prepared for U.S. Army Corps of Engineers, Sacramento Dist.*
- ASCE. (1975). *Sedimentation engineering, Manuals and Reports on Engineering Practice No. 54*, New York.
- Community Coalition for a Napa River Flood Management Plan. (1996). "The living river strategy, a community based plan for flood protection and watershed management." *Rep.*
- Cunge, J. A., Holly, F. M., and Verwey, A. (1980). *Practical aspects of computational river hydraulics*, Iowa Institute of Hydraulic Research, Iowa City, Iowa.
- DeTemple, B. (1998). "MARSH 98: Marsh plain evolution modeling." *Tech. Memo.*, Philip Williams & Associates, Ltd., Corte Madera, Calif.
- Doyle, J. (2000). "Napa breaks ground on 'radical' flood plan." *San Francisco Chronicle*, July 31.
- Egan, T. (1998). "For a flood-weary Napa Valley, a vote to let the river run wild." *New York Times*, April 25.
- Ellison, K. (2000). "Napa takes a unique approach to floods." *San Jose Mercury News*, July 31.
- Federal Emergency Management Agency (FEMA). (2000). "Project Impact: Building a disaster resistant community. Napa County, California." (http://www.fema.gov/impact/cities/im_ca04.htm).
- Fischer, H. B., List, E. J., Koh, R. C. Y., Imberger, J., and Brooks, N. H. (1979). *Mixing in inland and coastal water*, Academic, San Diego.
- Gibbs, R. J. (1987). "Sources of estuarine sediments and their coagulation." *Sedimentation control to reduce maintenance dredging of navigational facilities in estuaries*, National Academy Press.
- Intergovernmental Panel on Climate Change (IPCC). (1995). *Second assessment report: The science of climate change*, Cambridge University Press, London.
- Krone, R. B. (1962). "Flume studies of transport of sediments in estuarial

- shoaling processes." *Final Rep.*, Hydr. Engrg. Res. Lab., University of California, Berkeley, Calif.
- shoaling processes." *Final Rep.*, Hydr. Engrg. Res. Lab., University of California, Berkeley, Calif.
- Krone, R. B. (1987). "A method for simulating historic marsh elevations." *Proc., Spec. Conf. on Quantitative Approaches to Coastal Sediment Processes, Coast. Sediments '87*, 316–323.
- McDonnald, T. E., and Cheng, R. T. (1997). "A numerical model of sediment transport applied to San Francisco Bay, California."
- MIKE 11, A computer based modeling system for rivers and channels: Reference manual.* (1995). DHI Water and Environment.
- Neary, V. S., Williams, P. B., Goodwin, P., and Mead, A. (1996). "Preliminary analysis of a geomorphically-based channel design for the Napa River flood management plan." *PWA Rep. 1140 Prepared for U.S. Army Corps of Engineers, Sacramento Dist.*, Philip Williams & Associates, Ltd.
- Neary, V. S., Wright, S. A., Bereciartua, P., and Williams, P. B. (1997). "Sediment transport assessment for Napa River flood damage reduction project." *PWA Rep. 1185 Prepared for U.S. Army Corps of Engineers, Sacramento Dist.*, Philip Williams & Associates, Ltd.
- van Rijn, L. C. (1989). "Sediment transport by currents and waves." *Delft Hydr. Rep. No. 468*.
- Warner, J. C., Schladow, S. G., and Schoellhamer, D. H. (1999). "Summary and analysis hydrodynamic and water quality data for the Napa/Sonoma Marsh Complex, final report, equipment deployment from September 1997 to March 1998." *Envir. Dyn. Lab. Rep. No. 98-07*, University of California, Davis, Calif.
- Water Engineering & Technology, Inc. (WET). (1990). "Napa River sediment engineering study: Phase I and II." *WET Proj. No. 82-507-89*, Prepared for U.S. Army Corps of Engineers, Sacramento Dist.
- Wolman, M. G., and Miller, J. P. (1960). "Magnitude and frequency forces in geomorphic processes." *J. Geol.*, 68, 54–74.

NOTATION

The following symbols are used in this paper:

- A = cross-sectional flow area;
 C = cross-sectional average sediment concentration;
 c = local sediment concentration;
 c_b = bed load sediment concentration;
 D = flow depth;
 D^* = average depth through which particles settle;
 D_{50} = median particle diameter;
 K = dispersion coefficient;
 M^* = bed erodibility;
 Q = water discharge;
 Q_s = sediment discharge;
 q_s = suspended load transport per unit width;
 S_e = erosion flux;
 S_d = deposition flux;
 t = time;
 U = average cross-sectional flow velocity;
 U^* = average cross-sectional shear velocity;
 U_{cd} = critical deposition velocity;
 U_{ce} = critical erosion velocity;
 u = local velocity;
 W = width of cross section at water surface;
 w = particle settling velocity;
 x = longitudinal coordinate;
 z = vertical coordinate; and
 ϵ = sediment porosity.